

Optical spectroscopy of Fano interference in a GaAs/Al_xGa_{1-x}As superlattice in a magnetic field

G. Cohen, Hadas Shtrikman, and I. Bar-Joseph

Department of Physics, The Weizmann Institute of Science, Rehovot 76100, Israel

(Received 12 June 1995)

We report on the observation of Fano interference of excitons and continuum in semiconductor superlattices subjected to a magnetic field applied parallel to the layers. We demonstrate how by varying the strength of the magnetic field we are able to tune the energy of a spatially indirect exciton resonance relative to the continuum edge. We measure the transmission spectra and the four-wave-mixing decay patterns and show that both are significantly modified as the exciton crosses the continuum edge.

The coupling between a continuum of states and a discrete resonance is known to give rise to a unique absorption spectrum. When such a system is excited from a common ground state a destructive interference of the transition amplitudes of the resonance and the continuum occurs. This results in an asymmetrical absorption line shape, with a dip on one of its sides.¹ This phenomenon, named after Fano, is found in atomic systems,² bulk semiconductors,^{3,4} and low-dimensional structures.⁵ It was recently shown that Fano interference could have a profound effect not only in the spectral domain but also in the dynamics of the system.⁶

In this paper we investigate the energy spectrum and dynamics of excitons in a narrow-band superlattice subjected to a strong magnetic field parallel to the layers. We focus on the optical transition from a hole state in a certain well to an electron state in an adjacent well, forming a spatially indirect exciton. By varying the strength of the magnetic field we are able to tune the energy of that indirect exciton resonance relative to the continuum edge of the direct transition. This provides a unique opportunity to investigate Fano interference near the band edge. We find that the decay pattern of the time integrated four-wave-mixing (FWM) signal and the linear transmission spectra change significantly at the field where the resonance crosses the continuum edge. At that critical field the FWM signal abruptly develops an oscillatory behavior and the absorption peak of the indirect exciton transition starts to shift rapidly to higher energies. We present a simple model, based on the Fano formalism, which explains very well the observed behavior.

Narrow-band superlattices are characterized by an interwell coupling that is smaller than the exciton binding energy. In GaAs/Al_xGa_{1-x}As superlattices this condition is fulfilled when the miniband width is less than ~ 20 meV. In these structures the Coulomb potential created by the photoexcited hole substantially deforms the translation symmetry of the conduction miniband.⁷ The resulting energy spectrum of the excitonic states can be presented as depicted in Fig. 1(a). We shall term in the following the direct (intrawell) and indirect (interwell) excitons as D_{exc} and I_{exc} , respectively. Clearly, the binding energy of the D_{exc} is larger than that of the I_{exc} . We have previously shown that these excitons are observed as sharp features in the absorption spectrum.⁸

When a strong magnetic field is applied in a direction parallel to the layers of a superlattice it affects the electron tunneling across the barriers and modifies the energy spec-

trum of the band. One can define the strong magnetic field limit, where the electron cyclotron energy becomes comparable to and even larger than the miniband width.⁹ In narrow-band superlattices this limit can be reached using experimentally accessible fields, ≤ 10 T. To understand the energy spectrum of excitons in this limit let us first consider an electron in an isolated quantum well, while turning off the Coulomb interaction. Its wave function can be written as $\phi_{e1}(z)\exp(-ik_y y)\exp(-ik_x x)$ and the first-order correction to its zero-field energy is¹⁰

$$E^{(1)} = \frac{e^2 B^2}{2m^* c^2} \left(\frac{c\hbar k_y}{eB} - \langle z \rangle \right)^2 + \frac{e^2 B^2}{2m^* c^2} (\langle z^2 \rangle - \langle z \rangle^2), \quad (1)$$

where B is the applied magnetic field, z is the growth axis, and y is the direction normal to the field and parallel to the layers. The first term describes a parabolic dispersion of the electron energy as a function of its guiding center position $z_0 = c\hbar k_y / eB$. Using a tight-binding approach to describe the energy spectrum of an electron in a superlattice, this term gives rise to a family of intersecting parabolas, one for each

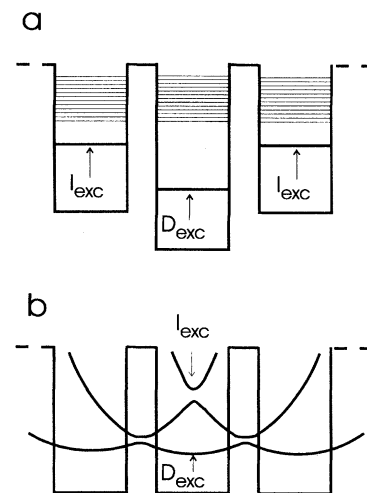


FIG. 1. (a) The electron energy levels (a) in a narrow-band superlattice in the presence of a hole and (b) in the presence of strong magnetic field. D_{exc} and I_{exc} designate the electron levels, which are involved in the direct and indirect excitons, respectively.

well. Tunneling mixes these curves and results in their anti-crossing, as shown in Fig. 1(b). The second term of Eq. (1) represents a simple diamagnetic shift common to all states, with no spatial dispersion.

Let us now turn on the Coulomb interaction. It can be easily shown that excitons can be formed by electrons, whose guiding centers are at the extrema of the energy dispersion curves, marked by arrows in Fig. 1(b). The wave functions of the I_{exc} electrons reside primarily at the left and right wells, and in that sense they form an indirect exciton. The magnetic field shifts the I_{exc} energy upward [Fig. 1(b)], until at some critical field its energy crosses the continuum edge of the D_{exc} . We define by Δ the difference in energy between the I_{exc} and the D_{exc} continuum edge,

$$\Delta = E(I_{\text{exc}}) - E(D_{\text{exc}} \text{ continuum}). \quad (2)$$

It follows that at zero magnetic field $\Delta < 0$, and at the critical field, where the I_{exc} crosses the D_{exc} continuum edge, $\Delta = 0$. From Fig. 1(a) it can be seen that $\Delta = 0$ occurs at a magnetic field that shifts I_{exc} by its binding energy. We shall present transmission and FWM data, which investigate the interaction between the I_{exc} resonance and the D_{exc} continuum in the vicinity of $\Delta = 0$.

The sample we studied is a GaAs/Al_xGa_{1-x}As superlattice grown by molecular-beam epitaxy. It is composed of 40 periods of undoped 93-Å GaAs wells and 22-Å Al_{0.45}Ga_{0.55}As barriers. It is sandwiched between two spacer layers consisting of 800 Å of undoped GaAs, grown on an n^+ ($2 \times 10^{18} \text{ cm}^{-3}$) GaAs buffer layer. The miniband width, calculated by a Kronig-Penney model, is 8 meV. The sample was glued to a thin glass slide and its back side was wet etched to allow transmission measurements. The optical experiments were performed in a magneto-optic cryostat at liquid-helium temperature, using a continuous-wave Styryl 8 dye laser and a mode-locked Ti:sapphire laser. The FWM experiments were carried out in a two beams geometry. In this geometry the two exciting beams propagate along the directions \mathbf{k}_2 and \mathbf{k}_1 and the time integrated signal along the $2\mathbf{k}_2 - \mathbf{k}_1$ direction was measured. The Ti:sapphire laser was optimized to have an autocorrelation and a spectral width of 150 fs and 20 meV, respectively.

In Fig. 2 we show three transmission spectra measured at 1, 3, and 6 T. The two large peaks at 1.556 and 1.574 eV are the heavy- and light-hole exciton transitions, respectively. A third smaller peak can be clearly observed at an intermediate energy value, 1.563 eV at 1 T. Following the behavior of this peak in an electric field normal to the layers we have identified it as an indirect exciton, formed by an electron and a hole, whose wave functions are centered in different wells.⁸ The binding energy of this exciton can be estimated to be ~ 2 meV.¹¹ In the above terminology the heavy-hole and the indirect exciton peaks correspond to the D_{exc} and the I_{exc} , respectively.

It can be seen that while the direct heavy- and light-hole excitons' positions shift only slightly between 1 and 6 T, < 1 meV, the I_{exc} exhibits a much larger shift, ~ 3 meV. The open circles in Fig. 3 describe the energy of the I_{exc} peak (relative to the D_{exc}) as a function of magnetic field. We observe a profound change around 3 T: while at low fields the I_{exc} relative position remains constant, it shifts quadrati-

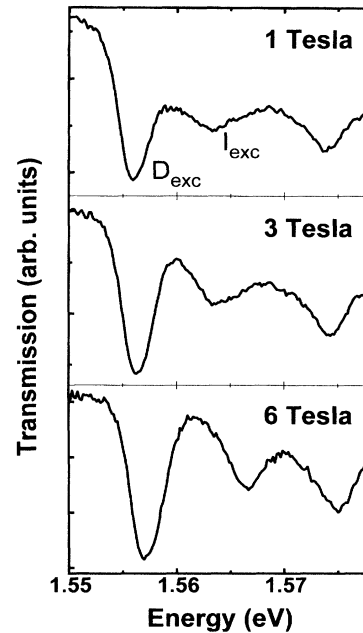


FIG. 2. Transmission spectra at magnetic fields of 1, 3, and 6 T applied parallel to the layers.

cally to higher energies above 3 T. The solid line in Fig. 3 describes the calculated energy difference between I_{exc} and D_{exc} , based on Eq. (1). It can be seen that there is very good agreement with the data points above 3 T. It should be noticed that the curvature of the line is determined by fundamental constants, and the only adjustable parameter is the energy difference at $B=0$, which is taken as 5.5 meV.¹² Clearly, the curve fails to describe the field dependence below 3 T.

Figure 4 shows FWM signals measured at different applied magnetic fields, with the excitation energy centered at 1.559 eV, covering the D_{exc} and the I_{exc} transitions. A qualitative difference between the low- and high-field signals is clearly observed. Below 3 T the overall decay is exponential, exhibiting a dip near zero time delay. An abrupt change in this behavior occurs at $B \geq 3$ T: fast oscillations appear in the decay pattern. The frequency of these oscillations increases

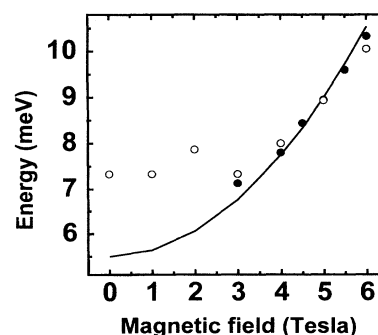


FIG. 3. The energy difference between I_{exc} and D_{exc} vs applied magnetic field: solid line, calculated; open circles, measured; the solid dots are the measured FWM oscillation frequencies.

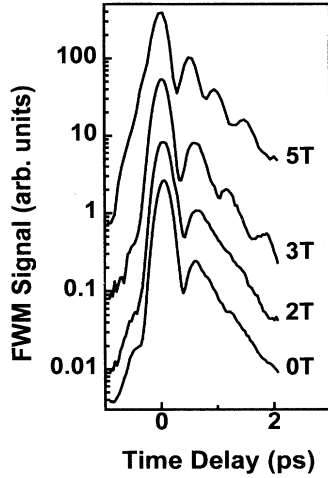


FIG. 4. FWM signals vs time delay at four different magnetic fields. The laser energy is centered at 1.559 eV.

quadratically with magnetic field, as shown in Fig. 3 (solid dots). It can be seen that this frequency matches the energy difference between the I_{exc} and D_{exc} (open circles). One can, therefore, conclude that the fast oscillations are quantum beats between the I_{exc} and D_{exc} excitons.

We now wish to discuss the experimental results, starting with the linear transmission data. It can be understood in terms of the interaction between a resonance and a continuum. This interaction causes each continuum state to be repelled from the resonance by an amount which depends on their relative energy separation. Consequently, there is a “pile-up” of continuum states, which forms a sharp absorption peak. At $\Delta < 0$, as the resonance is far below the continuum edge, the interaction is weak and effectively involves only the lowest continuum states. The resulting pile-up is not pronounced and the energy of the absorption peak is not very sensitive to small changes in the energy of the discrete level. When Δ becomes positive the interaction is enhanced and involves more continuum states. The absorption resonance becomes sharper and more sensitive to changes in the energy of the discrete state. This mechanism explains qualitatively the measured absorption line shapes (Fig. 2): the blueshift and narrowing of the I_{exc} peak and the different behavior of the I_{exc} below and above 3 T (Fig. 3).

To formulate it more quantitatively we consider a model where the I_{exc} is coupled to the D_{exc} continuum by tunneling. We write the wave functions of an electron in these two states assuming that the bound state is exponentially localized near the hole and the continuum is a plane wave. The I_{exc} wave function is then written as $\phi_{\text{ex}} = \phi(z)\exp(-k_{\perp}r)$ and that of a D_{exc} continuum state is approximated as $\psi_c = \psi(z)\exp(-ik_x x - ik_y y)$. The matrix element for coupling between these two states has, therefore, the form $\langle \phi(z)|v|\psi(z)\rangle \langle \exp(-k_{\perp}r)|\exp(-ik_x x - ik_y y)\rangle$, where v is the tunneling matrix element. The left bracket can be approximated as a constant¹³ and estimated to be $V \approx 4$ meV in our structure. The full coupling term, V_E , between the exciton and the continuum, taking into account the two-dimensional density of states and energy conservation, is therefore $V_E = 2VT/(E+T)^{3/2}$, where $T = \hbar^2 k_{\perp}^2 / 2m^*$. Note that the

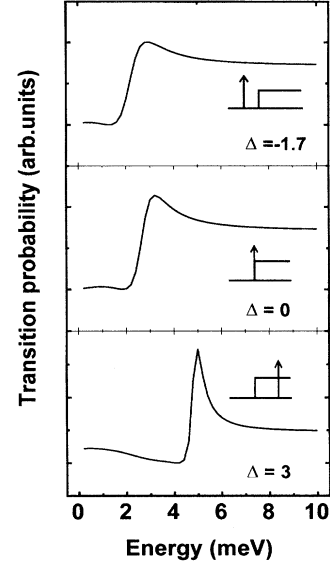


FIG. 5. Calculated Fano interference line shapes at three different values of Δ . Insets: energy position of the discrete level (arrow) relative to the continuum edge.

use of plane waves rather than the radial wave function to describe the continuum states leads to an overestimation of the coupling strength just above $E=0$. Therefore, this approximation gives an upper limit for the value of V_E .

We are now able to insert this coupling term into the Fano formalism¹ and calculate the absorption line shape. Figure 5 describes the evolution of the calculated absorption spectrum as we vary Δ . One can see the formation of a narrow resonance, which shifts to higher energies with increasing Δ , forming a shallow dip at its low-energy side. Notice that this shift is not linear in Δ , and is slow for $\Delta < 0$ and fast for $\Delta > 0$. At $\Delta \gg 0$ the increase of coupling strength between the continuum and discrete state gives rise to a broadening of the absorption resonance.

The above model implies that the absorption peak is not the bare I_{exc} but is rather a mixture of this resonance and the D_{exc} continuum. At low fields it has predominantly a continuum nature and at high magnetic fields this peak contains a larger excitonic contribution.

This mixed nature of the indirect exciton peak is consistent with the different decay patterns of the FWM signal below and above 3 T. We note that in the FWM experiment we excite simultaneously the D_{exc} and the I_{exc} peaks. Since FWM is a coherent process the signal will contain a contribution due to interference between the two transition amplitudes. The character of the I_{exc} , being continuumlike or excitonlike, determines the type of this interference: either between a resonance (D_{exc}) and continuum or between two resonances.

Let us consider first the low-field signal. It was shown by Feldman *et al.* that when an excitonic resonance and its continuum are coexcited in a FWM experiment, the resulting decay pattern is exponential with a dip just after zero time delay.¹⁴ This pattern is similar to the one observed in our experiment below 3 T. We can therefore conclude that in this field range the I_{exc} has a *continuum nature*. As we increase

the magnetic field the signal changes into quantum beats between two resonances. This implies that the I_{exc} peak contains a larger *excitonic contribution*. It should be noticed that the first minimum in the oscillatory signal is deeper than the others. This is due to the fact that the contribution of the continuum states to the absorption peak is not negligible.

Finally, we wish to remark on the dependence of the FWM decay times on the magnetic field. As we tune the laser to the low-energy side of the heavy-hole exciton we observe that the strength of the oscillations decreases, until they gradually disappear. Under these conditions we excite mainly the D_{exc} , and can therefore follow its dephasing. We observe a factor of 4 increase in the decay time of the signal, from 0.5 ps at 0 T to 2 ps at 6 T. To identify the origin of this

increase we performed a FWM experiment on a multiple-quantum-well sample, grown under the same conditions, with the same well width but wider barriers (100 Å). No change in the decay time was seen between 0 and 6 T. Furthermore, the decay time was found to be similar to the one measured in the superlattice sample at high fields, 2 ps. These observations suggest that the fast decay at low fields (0.5 ps) is related to the coupling between the wells, and the increase in decay time at high fields is due to localization of the exciton in a single well. Further work is needed to substantiate this conclusion.

This work was supported by the Minerva Foundation, Munich, Germany.

¹U. Fano, Phys. Rev. **124**, 1866 (1961).

²H. Beutler, Z. Phys. **93**, 177 (1935).

³D. S. Chemla, A. Maruani, and E. Batifol, Phys. Rev. Lett. **42**, 1075 (1979).

⁴S. Glutch, U. Siegner, M.-A. Mycek, and D. S. Chemla, Phys. Rev. B **50**, 17 009 (1994).

⁵D. Y. Oberli, G. Böhm, G. Weimann, and J. A. Brum, Phys. Rev. B **49**, 5757 (1994).

⁶U. Siegner, M.-A. Mycek, S. Glutch, and D. S. Chemla, Phys. Rev. Lett. **74**, 470 (1995).

⁷M. M. Dignam and J. E. Sipe, Phys. Rev. B **43**, 4097 (1991).

⁸G. Cohen, H. Shtrikman, and I. Bar-Joseph, Phys. Rev. B **50**, 17 316 (1994).

⁹T. Duffeld *et al.*, Phys. Rev. Lett. **59**, 2693 (1987).

¹⁰J. C. Maan, in *Physics and Applications of Quantum Wells and Superlattices*, edited by E. E. Mendez and K. von Klitzing (Plenum, New York, 1987), pp. 347–375.

¹¹T. Westgaard *et al.*, Phys. Rev. B **45**, 1784 (1992).

¹²This value implies binding energies of 7.5 and 2 meV for the direct and indirect excitons, respectively.

¹³S. A. Gurvitz and S. Marinov, Phys. Rev. A **40**, 2166 (1989).

¹⁴J. Feldmann *et al.*, Phys. Rev. Lett. **70**, 3027 (1993).